Evolution of a strongly correlated liquid with electronic density

X. Wang,[1,2] C. A. Burns,[1] A. H. Said,[1,3] C. N. Kodituwakku,[1,3] Y. V. Shvydko,[3] D. Casa,[3] T. Gog,[3] and P. M. Platzman[4]
[1]*Department of Physics, Western Michigan University, Kalamazoo, Michigan 49008, USA*
[2]*Department of Physics, Hebei University of Engineering, Handan, Hebei Province 056038, China*
[3]*XOR, Advanced Photon Source, Argonne National Laboratory, Argonne, Illinois 60439, USA*
[4]*Bell Labs, Alcatel-Lucent, Murray Hill, New Jersey 07974, USA*
(Received 11 June 2009; revised manuscript received 13 December 2009; published 2 February 2010)

Systems created by dissolving elemental metals in liquid ammonia are strongly correlated liquid metals where the electronic correlation strength can be easily changed by altering the electronic density. We study the plasmon in the lithium ammonia system as a function of electronic density using nonresonant inelastic x-ray scattering and use this to determine the long wavelength plasmon energy E_0 and the plasmon dispersion α as a function of electronic density. These parameters show the increasing influence of electronic correlations as we go to lower concentrations. The plasmon width is found to increase as we go to lower concentration. The implications of these results are discussed.

DOI: 10.1103/PhysRevB.81.075104 PACS number(s): 71.45.Gm, 78.70.Ck

I. INTRODUCTION

Systems with strong electronic correlations are an area of great theoretical and experimental interests. Metal ammonia systems[1] are a fascinating example of a highly correlated system with a low electronic density which can be easily varied. These systems are formed by dissolving elemental metals in liquid ammonia. Many alkali (Li, Na, K, and Cs) and alkaline earth metals (Ca, Sr, and Ba), as well as some lanthanoids (Eu and Yb), can be dissolved to high concentrations. The metal atoms ionize, resulting in one (in the case of alkali metals) or two (for other metals) unbound electrons and a charged positive ion. The electronic concentration can be altered by simply changing the amount of dissolved metal. A recent review, concentrating on calculations of the properties of the solutions, has been given by Zurek *et al.*[2]

Figure 1(a) shows the phase diagram for the lithium ammonia mixtures which are studied here. At low concentrations the electrons are trapped in cavities formed by the polar ammonia molecules, while at high concentrations they delocalize to create a good liquid metal. Between these two states they undergo a metal to insulator transition (MIT). An overview of the MIT in these systems is given by Mott.[3] In the region of the MIT, a change in the electronic concentration by a factor of 2 alters the conductivity by about three orders of magnitude. There is also a liquid-liquid phase separation, where the mixture spontaneously separates into macroscopic metallic and insulating regions with the lighter metallic region floating on top. Lithium ammonia saturates at about 20 mol % metal (MPM). The color of the mixtures varies from deep blue to golden yellow as the concentration increases. A true solid compound, $Li(NH_3)_4$, is formed with a melting temperature of 89 K, which is lowest melting temperature of any metal.

The electron density helps us to determine the properties of the electronic interactions, which play a major role in the solution properties. The electronic density is usually written as

$$r_s = \frac{\left(\frac{4}{3}\pi n\right)^{-1/3}}{a_0^*}, \tag{1}$$

where n is the free electron density and a_0^* is the effective Bohr radius. $a_0^* = \hbar^2\varepsilon/m^*e^2$, where m^* is the effective mass of

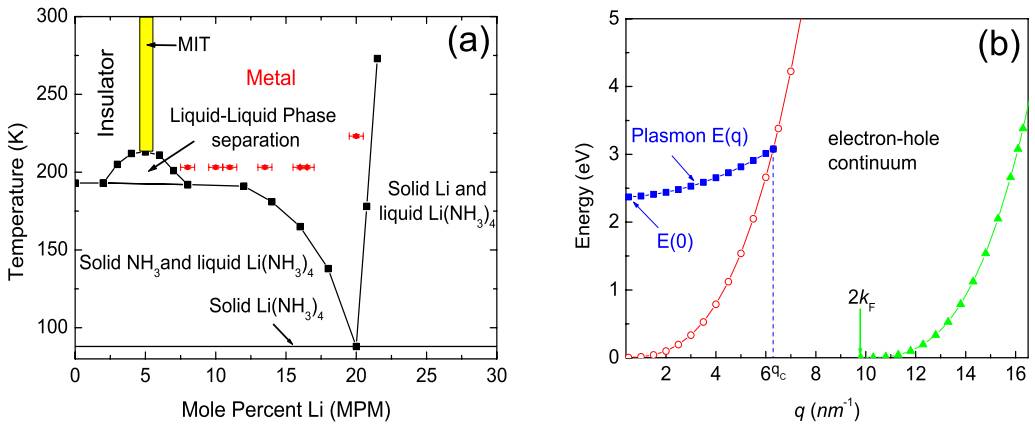

FIG. 1. (Color online) (a) Phase diagram for liquid lithium ammonia mixtures. Samples discussed in the text are indicated by the dots on the diagram. (b) Energy dispersion and electron-hole continuum RPA calculation for a plasmon with the electronic density seen at 20 MPM. At the cutoff momentum transfer q_c, the plasmon decays to electron-hole excitation.

the electron and ε is the static dielectric constant. Since the Coulomb energy is proportional to $1/r_s$ while the kinetic (Fermi) energy is proportional to $1/r_s^2$, r_s is approximately the ratio of Coulomb to kinetic energies for electrons in a uniform electron gas at zero temperature. r_s is also proportional to the separation between electrons, so large values of r_s correspond to small electron densities and a small role for the kinetic energy. Typical elemental metals have $2<r_s<6$, while lithium ammonia solutions are metallic for values $7.35<r_s<11.3$ (assuming that the effective Bohr radius is the same as the standard Bohr radius). At higher values of r_s the systems become insulating, and r_s increases toward infinity when lithium concentrations approach zero. In this paper, the samples we studied have values of r_s from 7.85 (16 MPM) to 9.60 (8 MPM).

Several scattering studies have shed light on the role of the electrons in these materials. High energy resolution inelastic x-ray scattering has been used to measure[4] the dispersion for the acoustic collective excitations for lithium and sodium ammonia solutions at several concentrations. These measurements showed a well-defined phononlike excitation to large momentum transfers and a softening in the dispersion near twice the Fermi wave vector.[5] Neutron studies[6] have also reported such a sharpening. Departures from the Bohm-Staver model for electron-ion coupling were found as well.[4] Other work in this system has studied the correlations by examining the properties of the plasmon at several electronic densities, as well as in the solid state.[7–9] Deviations from the random phase approximation (RPA) were reported and linewidths of plasmon peaks in this system were discussed. Here we extend the earlier work to lower concentrations and use the wider range of densities to extract the functional dependences of the plasmon parameters with density. Earlier electron energy loss spectroscopy measurements[10] of the plasmon properties in simple alkali metals showed unexpectedly strong deviations from RPA even at low values of r_s, and the metal ammonia systems provide another opportunity to study such effects.

A simple starting model for the behavior of electrons in solids is the jellium model, where the electron interactions can be approximately treated using the RPA. In the RPA, the electron interactions are treated by assuming that the actual correlation seen by an electron is equal to the average effect due to all the other electrons. While this model should be very accurate at high concentrations and long wavelengths, as the electronic density gets low it becomes inadequate. In fact, at sufficiently large values of r_s the electrons will localize to form the so-called Wigner crystal. Monte Carlo calculations indicate that such a crystal should occur when $r_s \sim 100$ in three dimensions.[11]

RPA predicts that the plasmon energy at zero momentum transfer is

$$E_0 = \hbar\omega_p = \hbar\left(\frac{4\pi ne^2}{\varepsilon m^*}\right)^{1/2}. \tag{2}$$

Here, m^* and ε may differ from the true electron mass m_e and the free space dielectric constant ε due to interactions in the medium. There exists a critical wave vector q_c above which the plasmon is no longer well defined since it can decay into an electron-hole pair. Figure 1(b) is a schematic drawing of the expected behavior. Here,

$$q_c \approx \omega_p/v_F, \tag{3}$$

which means that when the particle velocity v_F is comparable to the phase velocity of the plasmon, it can decay into electron-hole excitations. While the jellium model does well at low energies and low values of r_s, it may be inadequate for the samples described here.

For momentum transfer $q<q_c$, RPA predicts the plasmon dispersion relationship,

$$E(q) = E_0 + \frac{\hbar^2}{m_e}\alpha q^2 + O(q^4). \tag{4}$$

Terms beyond the quadratic will provide only a small correction to the energy and will not be considered here. The dispersion of the plasmon is due to the electron-electron interactions, and a measurement of α gives information about the strength of these interactions. RPA predicts that α is a coefficient that depends only on the electron density,

$$\alpha = \frac{3E_F}{5E_0} \propto n^{1/6}. \tag{5}$$

Within RPA, the coefficient α is completely determined by E_F and E_0; that is, even if we do not know the dielectric constant or the effective mass, if we determine the plasmon energy at $q=0$ we fix the coefficient α within RPA.

It is known that the RPA will break down at sufficiently large values of r_s; in fact, the RPA predicts that the electron gas will show a negative compressibility at about $r_s \sim 5.24$ (see, for example, Ref. 12). Matsuda *et al.* used x-ray diffraction and small angle x-ray scattering to study expanded liquid rubidium as a function of electronic density.[13] They observe a variation in density which may indicate enhanced ionic attraction at $r_s \sim 5.25$ which they suggest is related to the instability of the electron gas.

II. EXPERIMENTAL DETAILS

Samples of lithium ammonia with concentrations from 20 to 8 MPM were prepared. These solutions correspond to electron densities from $4.1\times10^{21}e^-$ to $1.8\times10^{21}e^-$ cm^{-3}. Pure lithium metal (99.9%) was weighed in a glovebox under an argon atmosphere and then placed in the sample cell still under argon. The valve to the cell was closed off, and it was attached to a gas handling system where electronic grade (99.999%) ammonia was condensed into the cell at a temperature of about −70 °C. The amount of gas condensed was determined using the known volume of the gas handling system, the temperature, and the pressure drop in the system. Once the sample was complete, the cell was sealed off and stored in liquid nitrogen until the experiment. We estimate an uncertainty in the concentration based on the error in creating the materials of ~0.5 MPM. Data were taken at 20, 16, 11, 10, and 8 MPM.

The samples discussed here cover a large change (~56%) in electronic density—for comparison, if pure lithium metal is compressed to 10 GPa the electronic density is increased by ~35%.[14] In addition, while pressure increases the electronic density, diluting the solution reduces the electronic density. Electronic correlations are generally largest at low electronic densities, so going to lower densities is of interest to us for this reason.

Inelastic x-ray scattering measurements were taken at the medium energy resolution spectrometers on beamlines 9-ID (20 MPM) and 30-ID (16, 11, 10, and 8 MPM) at the Advanced Photon Source in a near backscattering geometry. A more detailed description of the instrument at sector 9 is given elsewhere[15] and is generally similar to the spectrometer at sector 30. However, the spectrometer at sector 30 incorporates a position sensitive detector based on the scheme of Huotari *et al.*[16] This design allows for collection of multiple energies with a higher solid angle and so greatly enhances the count rate. The total energy resolution of the spectrometers was about 110 meV and the q resolution was set to be 0.6 nm^{-1} by appropriate slits on the analyzer. X rays entered and exited the sample cell through thin (0.25 mm) Be windows which were epoxied to the front and back of the rectangular cell. The epoxy (Varian Torr-Seal) had been previously tested and found not to react with the solutions. Measurements on representative samples were repeated several times and showed identical results indicating no alternation in the sample quality over time. We also compare our results with data taken earlier[7,8] at 20, 16.5, and 13 MPM.

For measurements, sample cells were transferred from dry ice to a precooled close cycle refrigerator kept at a temperature of −70 °C. Data were also taken at this temperature. Typically a cell could be transferred and cooled in less than a minute. Warming of the fridge during the transfer was less than 1 °C. Temperature stability during the measurements was better than 0.5 K. The windows on the close cycle refrigerator were sufficiently transparent to allow visual observation of the cell; in some cases a small amount of frost condensed on the cell during the transfer, but this quickly evaporated in the vacuum.

III. DATA AND ANALYSIS

X-ray measurements[17] of the static structure factor $S(q)$ of lithium ammonia solutions with different concentrations are shown in Fig. 2. Detailed studies of the structure factor have also been carried out using neutron scattering by Wasse *et al.*[18] The ability to use the different scattering factors for different isotopes allows the neutron studies to determine the partial structure factors due to the different components. The peak near 10 nm^{-1} is related to the distance between the lithium atoms and is absent in $S(q)$ measurements for pure ammonia. It moves to lower q values as the lithium concentration is reduced and the lithium atoms move further apart. A lithium ion will form a complex with four ammonia molecules which increases the ordering and therefore the scattering. This ordering causes the first peak to become stronger than the second peak at higher concentrations. The peak near 20 nm^{-1} is related to the distance between the nitrogen atoms in the ammonia molecules and its position does not change dramatically with concentration. This peak is higher at the low concentrations due to the larger amount of ammonia per unit volume in the sample. By measuring the static structure factor on our samples and comparing to the previous measurements, we were able to verify the concentrations of the solutions and be sure that the concentrations did not change over time.

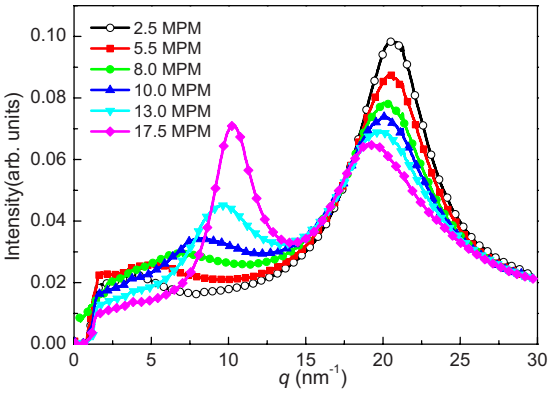

FIG. 2. (Color online) Structure factor for lithium ammonia solutions (Ref. 17). The first peak is related to the distance between the lithium atoms. It is near 10 nm^{-1} for the concentrated solution and moves to lower q values as the lithium concentration is reduced. The second peak near 20 nm^{-1} is related to the distance between the nitrogen in the ammonia molecules. At low concentrations, elastic scattering is larger at the q values where the plasmon exists.

Measurements of the plasmon at lower concentrations become progressively more difficult for several reasons. First, the scattering is proportional to the number of valence electrons in solution and is therefore reduced at low concentration. Second, the plasmon energy is lower [see Eq. (2)], which moves its position closer to the elastic line where the background is higher. Also, as shown in Fig. 2, the static structure factor $S(q)$ of lower concentration lithium ammonia solutions is larger at the q values (below 6 nm^{-1}) where we are looking for the plasmon. This scattering is mostly elastic and increases the background against which the plasmon must be measured. Finally, as will be discussed later, the plasmon width increases at low concentrations making it more difficult to distinguish from the background.

Figure 3 shows data at 16 MPM and illustrates the general properties of the plasmon. The plasmon peak grows in intensity, widens, and disperses to higher energies as the q value increases. Above q_c the plasmon broadens rapidly and quickly becomes difficult to distinguish from the background. From the matrix elements in the f-sum rule[19] the plasmon's integrated intensity is expected to increase roughly as q^2 (assuming that most of the spectral weight is in the plasmon). Changes in the path length through the sample at the different angles and the finite size of the analyzer crystal also must be accounted for. Since it is a result of the sum rule, the integrated intensity increases do not provide any new physical insights, so we concentrate on the position and width.

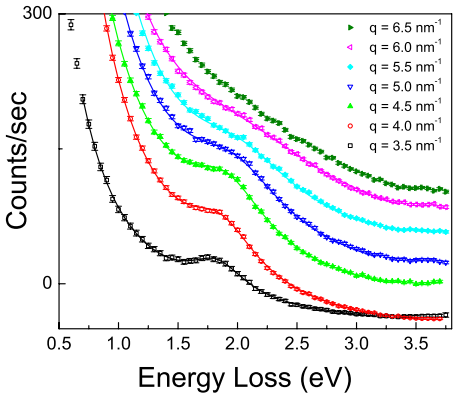

FIG. 3. (Color online) The plasmon at 16 MPM. The peak disperses to higher energies at higher q values as expected. In addition, the width of the peak increases. Above the cutoff vector $q_c \sim 0.61$ nm^{-1} the plasmon can decay into electron-hole pairs and it broadens rapidly.

The plasmon data for 10 and 11 MPM solutions are shown in Fig. 4. The plasmon signal has become significantly weaker. At these lower concentrations the plasmon becomes increasingly difficult to observe compared to the background. The insets in the graphs are the plasmon peaks after the background has been subtracted. The insets show the plasmon dispersing and becoming wider with q, qualitatively similar to the data at 16 MPM.

Some data taken at 8 MPM are shown in Fig. 5. These data were at one of the most favorable q values for seeing a plasmon above the background. The background increases with q (as does the width), but at low q the intensity is low from the sum rule. The low signal to background made it impossible for us to extract the plasmon properties with any confidence at the other q values, so we could draw few conclusions at this density.

Determination of the plasmon parameters requires accurate fitting to the data. The tail of the quasielastic

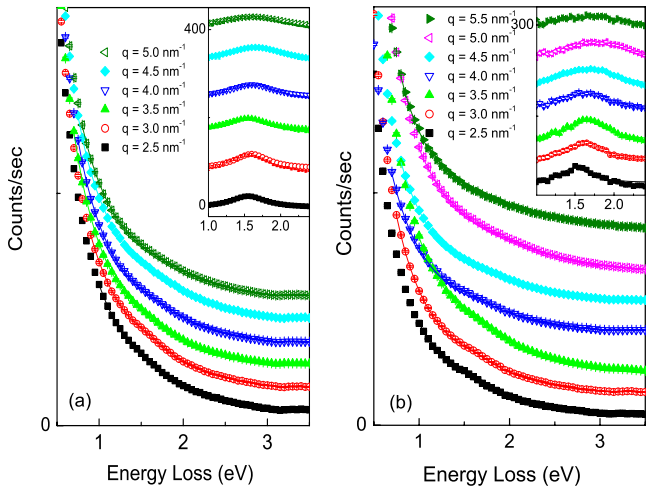

FIG. 4. (Color online) Plasmon data for (a) 10 MPM lithium ammonia solution and (b) 11 MPM lithium ammonia solutions. Insets show the data in the region of the plasmon with the elastic background subtracted. Fits to the data are the solid lines in the figures. The peaks are quite broad everywhere they are visible.

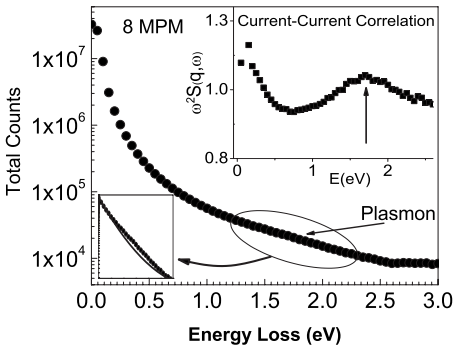

FIG. 5. Plasmon at 3.6 nm^{-1} in an 8 MPM solution. The region of the plasmon is circled and enlarged, showing a small deviation from the background. A peak is more visible in the inset which shows the current-current correlation function. The small rise above 2.6 eV is an instrumental artifact which occurs with the strip detector for the points near the end of a scan.

peak provides the background against which we measure the plasmon. Our instrumental resolution function is well approximated by a pseudo-Voigt function, that is, a weighted sum of Gaussian and Lorentzian contributions. The plasmon peak occurs at an energy which is many times the resolution width; at these energies the Gaussian contribution to the peak has essentially disappeared. This results in a background well approximated by a Lorentzian. We therefore fit our data to two Lorentzian models, one representing the plasmon and the other the background. The width of the plasmon is much greater than the instrumental resolution, so the plasmon's functional form is essentially unaffected by the resolution function of the instrument.

As a check on the accuracy of the fitting, we have also carried out fits using the current-current correlation function[20] which is defined as $C_L(q,\omega)=\omega^2 S(q,\omega)$. Here q is the momentum transfer, ω is the frequency of photons, and $S(q,\omega)$ is the dynamic structure factor of the material measured. The factor ω^2 reduces the low frequency portion of the structure factor and emphasizes the inelastic features of dynamic structure factor $S(q,\omega)$. With this method, it is easy to locate the peak positions in $S(q,\omega)$. Fits to the data at 8 MPM were only reliable using the current-current correlation function. The two types of fitting gave consistent results at the other concentrations. Solid lines in Figs. 3–5 show the range we fit over and the accuracy of the fits.

Figure 6(a) shows dispersion of plasmon energy for different concentration lithium ammonia solutions. The solid lines are the best fits to Eq. (4) and fit lines are drawn only out to the limit of the fitting range, that is, to q_c. The values of the cutoff momentum q_c are 6.3, 6.1, 5.8, and 5.7 nm^{-1} for 20, 16, 11, and 10 MPM, respectively. We only fit data in which none of the analyzer was seeing $q > q_c$. The plasmon energy and dispersion are both clearly reduced as the electron concentration is lowered.

Figure 6(b) shows the plasmon energy E_0 from our data compared with the predicted value using the RPA. The data in the figure at 13, 16.8, and 20 MPM were reported in earlier work.[7,9] The value for E_0 is clearly reduced, which is likely due to one or both of the terms in Eq. (2) related to the dielectric constant or effective mass (E_0 are listed with cor-

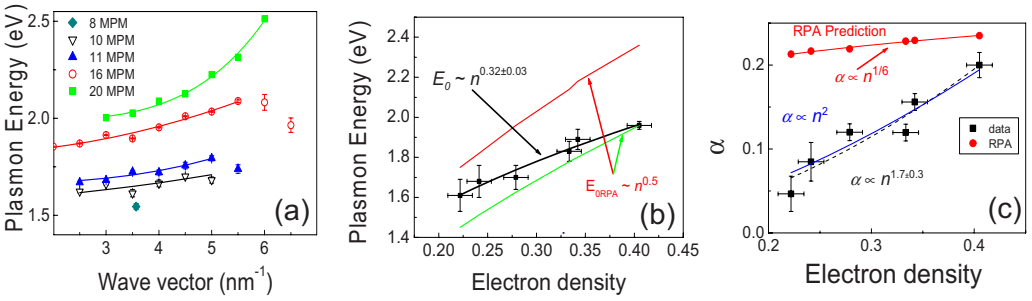

FIG. 6. (Color online) (a) Dispersion of plasmon energy for different concentration lithium ammonia solutions. The solid lines are the best fits to Eq. (4) to quadratic order. The fit lines are drawn only out to the points which were fit, that is, to q_c. (b) Plasmon energy vs electron density. In addition to our data, data from previous work [Eq. (9)] are included. The top solid curve is the prediction for the plasmon energy from RPA. The lower solid curve has the RPA functional dependence but that starts from the measured data point at 20 MPM. Both these curves have the same functional dependence and assume that the dielectric constant and effective mass remain constant. (c) Dispersion coefficients compared to RPA prediction. The black squares with error bars are the data for different electron concentrations. The dashed line is the best fit of experimental data to a power law dependence. Note the strong deviation from RPA.

responding concentrations in Table I). The reduction from the predicted plasmon energy is small, which provides support for the idea that the nearly free electron gas is a reasonable starting point for these materials.

From Eq. (2), we expect that $E_0 \propto n^{0.5}$. However, our data are best fit by an exponent of 0.32 ± 0.03 instead of 0.5. From Eq. (2), there is some ambiguity in the value of E_0 since the dielectric constant and the effective mass are unknown. The long wavelength energy of the plasmon is unlikely to change due to correlations. The most likely explanation for the different functional dependence is an alteration with density of either the dielectric constant or the effective mass of the electrons. As the electronic concentration is increased, we find that the E_0 values are becoming *closer* to the RPA values. This means that either the static dielectric constant or the effective mass is becoming smaller. Since they enter as a product we cannot specify how they are changing, but their behavior is a bit puzzling. As we go to lower concentrations we would expect the effective mass to stay the same or get larger since at the MIT transition the electrons will become localized. Similarly, based on capacitive measurements,[21] the static dielectric function for ammonia is fairly large, ~25 at a temperature of −70 °C. As we move to lower lithium concentrations we will eventually expect ε to approach this value and it seems likely it would increase as well. We unfortunately do not have an explanation for this result.

Figure 6(c) shows the dependence of the plasmon dispersion coefficient on the electronic density. A weak increase in the coefficient α with electron density is expected in the RPA from the definition of $\alpha = 3E_F/5E_0 \propto n^{1/6}$. However, the best fit to our data (plotted in the figure) that yields to a power law function of this form yields a value for the exponent of 1.7 ± 0.3. We show the best fit for an exponent of 2 in the figure as well. Clearly, the RPA treatment of the interactions is inadequate; the predicted exponent is off by more than one order of magnitude. Since electronic correlations act to reduce α, this drop-off is a clear signal of the increasing importance of the correlations in these systems and the failure of the RPA.

Note that while our data are consistent with Hiyashi *et al.*,[8] they concluded that their dispersion data indicated reasonable agreement with RPA. However, in Eq. (5) for the dispersion, they incorrectly used the RPA prediction with $\varepsilon = 1$ and $m^* = 1$, which is inconsistent with their measured value of E_0 [see Eq. (2)]. Our conclusions therefore differ from theirs.

Figure 7 shows the width of the plasmons. Plasmons in a wide variety of materials are found to have a width which cannot be explained within a jellium model.[22] While there is

TABLE I. Concentrations, electron densities, r_s values, and plasmon energies at zero momentum transfer (E_0).

Density (MPM)	Electron density $(n) \times 10^{22}$ (cm^{-3})	r_s	E_0 (eV)	E_0 error (eV)
8	0.1819	9.60		
10	0.2218	8.99	1.61	0.08
11	0.2413	8.74	1.68	0.08
13[a]	0.2789	8.33	1.7	0.06
16	0.3334	7.85	1.83	0.05
16.5[a]	0.3422	7.78	1.89	0.05
20[a]	0.4051	7.36	1.96	0.02

[a]Data from previous work.

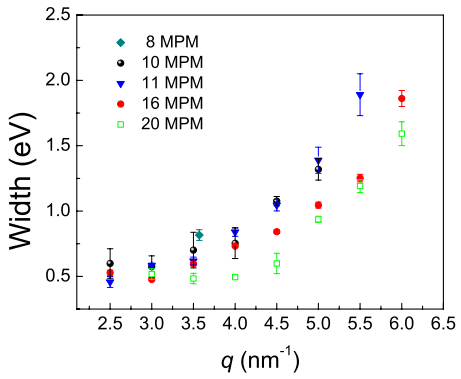

FIG. 7. (Color online) Plasmon width as a function of q. The plasmon width increases as the electronic concentration is reduced.

a probability for the plasmon to decay into two electron-hole pairs, calculations[23] of the width due to this effect are about one order of magnitude smaller than the measured results for simple metals. The width of the plasmon at $q=0$ can be shown to be proportional to the square of the Fourier transform of the pseudopotential in a nearly free electron model.[24] This implies an increase in the pseudopotential as we go to lower electronic densities. Such an increase is reasonable if the screening of the electrons decreases, which is expected as we go toward lower concentrations and the MIT. However, it should be noted that an accurate treatment of the problem requires an explicit treatment of the band structure in the material.[25]

There are several aspects of the jellium model that might not be adequate for these systems. One is that the jellium model does not treat inhomogeneities in the background charge distribution, that is, the band structure.[8] Substantial deviations in the dispersion coefficient from RPA predictions are found in the heavier alkali systems,[10] but much of this effect is due to the band structure in the metals.[26] Studies by Hill *et al.*[27] looked at the plasmon in both the liquid and solid phases of lithium and sodium and found that the only change in dispersion was consistent with the slight change in density of the systems. This seems to be an indication that the local order in the liquid favors similar states as the long-range order in the solid.

However, in the lithium ammonia system introducing long-range order by freezing a 20 MPM solution substantially altered the plasmon dispersion.[9] The deviation from RPA observed in the solid was consistent with alkali metal solids but substantially more than was observed in the liquid. There are two possibilities for the change in the solid, the change in the density (about 20%) or a difference in band structure. Since a higher electronic density should have better agreement with RPA and worse agreement is seen, it seems something else must be the cause.

It seems likely that the band structure effects may be quite different in the liquid than in the solid for lithium ammonia. In the alkali metals, the electrons occupy *s*-like wave functions. Such wave functions are likely to be fairly robust and may remain similar even in the liquid. Calculations for solid $Li(NH_3)_4$ indicate *f*-like states for the conduction electrons.[28] It seems likely that such states may be altered in the liquid, especially due to the rotational disorder which is present.

A third way in which the jellium model can be inadequate is if the electron density is not uniform. Monte Carlo studies[28] found that the electrons in solid $Li(NH_3)_4$ were not uniformly distributed but instead tended to "wet" the hydrogen atoms. Intrinsically, some additional variation in the electron density is likely, especially at lower electronic densities. The lithium atoms are coordinated by four ammonia molecules. At 20 MPM, this results in a uniform mixture of coordinated lithium ions. However, as the lithium concentration is reduced, the number of unassociated ammonia molecules increases. This results in a two-fluid mixture of pure ammonia molecules and charged lithium ammonia complexes. It is therefore quite likely that the electron density also varies in the medium.

In the case of a nonuniform electron distribution, the plasmon dispersion becomes more complicated. At plasmon wavelengths which are much longer than the electron density modulation, the plasmon properties would not be substantially affected. However, as we look at the scattering of x rays at larger wave vectors we are probing smaller distances. The relevant length scale is $1/k \sim 0.2$ nm for the case of a wave vector of 5 nm^{-1}.

We assume that the conduction electrons have high and low density regions, with densities ρ_h and ρ_l and fractional volumes v_h and v_l. We also have the condition that

$$\rho_h v_h + \rho_l v_l = \rho, \tag{6}$$

where ρ is the average electronic density of the system. For a simple illustrative case we consider only two regions, one with low electronic density and the other with a high electronic density. At wavelengths long compared to the electronic density variation, the behavior is that of the average electronic density. In this case the plasmon frequency at a wave vector q_l is given by Eq. (4) with E_0 and α given by Eqs. (2) and (5), respectively, using the average density. However, at large q_l the case is different. Now the x ray is sampling either a region of low electronic density or one of high electronic density. This will yield two solutions to Eqs. (2), (5), and (6), one for high and one for low density. In the limit where $\rho_l \rightarrow 0$, we recover a single plasmon in the high q limit, but now the parameter yields a larger value for the plasmon energy since $\rho_h > \rho$. The entire dispersion curve is therefore altered and the higher energy at the higher q leads to a larger apparent dispersion coefficient α. For small but nonzero values of ρ_l the weak signal and the low energy would make a second plasmon peak unobservable.

Nonuniform electronic density can therefore alter the apparent plasmon dispersion (and is also likely to alter the plasmon widths especially at the intermediate wave vectors). If the electron gas is inhomogeneous, testing models of the RPA becomes more difficult and will require an understanding of the electron distribution. It is important to note that the inhomogeneous electron distribution will lead to *higher* apparent dispersion for the plasmon, that is, values closer to the RPA prediction. So the results for the deviation from RPA are an upper bound; the true dispersion may be lower than what is derived from the simple jellium model.

IV. CONCLUSION

The ability to tune the electronic concentration over a wide range makes the metal ammonia systems interesting for studies of electronic correlations. We have carried out inelastic x-ray scattering measurements of the plasmon in lithium ammonia solutions as a function of electron concentration. The plasmon becomes broader and its dispersion decreases rapidly as we go to lower concentration. We find the density dependence of the exponent of the dispersion coefficient to be larger by one order of magnitude than predicted by the RPA, suggesting a strong increase in the importance of electronic correlations as the density is decreased. The plasmon width increases at lower concentration is consistent with a reduction in screening and behavior that is further removed from a nearly free electron gas.

ACKNOWLEDGMENTS

This work was supported by the Division of Materials Science, DOE under Grant No. DE-FG02-99ER45772. Use of the Advanced Photon Source at Argonne National Laboratory was supported by the Office of Basic Energy Sciences, U.S. Department of Energy under Contract No. DE-AC02-06CH11357. C.A.B. would like to thank K. B. Lee and POSTECH for their hospitality during his sabbatical year when the writing of this paper took place.

[1] See, for instance, J. C. Thompson, *Electrons in Liquid Ammonia* (Clarendon Press, Oxford, 1976).
[2] E. Zurek, P. P. Edwards, and R. Hoffmann, Angew. Chem., Int. Ed. **48**, 8198 (2009).
[3] N. Mott, *Metal-Insulator Transitions*, 2nd ed. (Taylor & Francis, London, 1990).
[4] A. H. Said, C. A. Burns, E. E. Alp, H. Sinn, and A. Alatas, Phys. Rev. B **68**, 104302 (2003).
[5] C. A. Burns, P. M. Platzman, H. Sinn, A. Alatas, and E. E. Alp, Phys. Rev. Lett. **86**, 2357 (2001).
[6] F. Sacchetti, E. Guarini, C. Petrillo, L. E. Bove, B. Dorner, F. Demmel, and F. Barocchi, Phys. Rev. B **67**, 014207 (2003).
[7] C. A. Burns, P. Abbamonte, E. D. Isaacs, and P. M. Platzman, Phys. Rev. Lett. **83**, 2390 (1999).
[8] H. Hayashi, Y. Udagawa, C.-C. Kao, J.-P. Rueff, and F. Sette, J. Electron Spectrosc. Relat. Phenom. **120**, 113 (2001).
[9] C. A. Burns, P. Giura, A. Said, A. Shukla, G. Vankó, M. Tuel-Benckendorf, E. D. Isaacs, and P. M. Platzman, Phys. Rev. Lett. **89**, 236404 (2002).
[10] J. Sprösser-Prou, A. vom Felde, and J. Fink, Phys. Rev. B **40**, 5799 (1989).
[11] D. M. Ceperley and B. J. Alder, Phys. Rev. Lett. **45**, 566 (1980).
[12] C. Bowen, G. Sugiyama, and B. J. Alder, Phys. Rev. B **50**, 14838 (1994).
[13] K. Matsuda, K. Tamura, and M. Inui, Phys. Rev. Lett. **98**, 096401 (2007).
[14] B. Olinger and J. W. Shaner, Science **219**, 1071 (1983).
[15] J. P. Hill, D. S. Coburn, Y.-J. Kim, T. Gog, D. M. Casa, C. N. Kodituwakku, and H. Sinn, J. Synchrotron Radiat. **14**, 361 (2007).
[16] S. Huotari, Gy. Vankó, F. Albergamo, C. Ponchut, H. Graafsma, C. Henriquet, R. Verbeni, and G. Monaco, J. Synchrotron Radiat. **12**, 467 (2005).
[17] P. Giura, C. A. Burns, R. Angelini, and M. De Michiel (unpublished).
[18] J. C. Wasse, S. Hayama, S. Masmanidis, S. L. Stebbings, and N. T. Skipper, J. Chem. Phys. **118**, 7486 (2003).
[19] L. X. Benedict and E. L. Shirley, Phys. Rev. B **59**, 5441 (1999).
[20] See, for instance, T. Scopigno, U. Balucani, G. Ruocco, and F. Sette, J. Phys.: Condens. Matter **12**, 8009 (2000).
[21] G. Billaud and A. Demortier, J. Phys. Chem. **79**, 3053 (1975), and references within.
[22] See, for instance, H. Raether, *Excitations of Plasmons and Interband Transitions by Electrons* (Springer-Verlag, New York, 1980).
[23] M. E. Bachlechner, H. M. Böhm, and A. Schinner, Physica B **183**, 293 (1993).
[24] G. Paasch, Phys. Status Solidi **38**, A123 (1970).
[25] W. Ku and A. G. Eguiluz, Phys. Rev. Lett. **82**, 2350 (1999).
[26] A. A. Quong and A. G. Eguiluz, Phys. Rev. Lett. **70**, 3955 (1993).
[27] J. P. Hill, C.-C. Kao, W. A. C. Caliebe, D. Gibbs, and J. B. Hastings, Phys. Rev. Lett. **77**, 3665 (1996).
[28] J. Kohanoff, F. Buda, M. Parrinello, and M. L. Klein, Phys. Rev. Lett. **73**, 3133 (1994).